Characterization of spike glycoprotein of 2019-nCoV on virus entry and its immune cross-reactivity with spike glycoprotein of SARS-CoV

CURRENT STATUS: UNDER REVIEW

nature research

Xiuyuan Ou
NHC Key laboratory of Systems Biology of Pathogens, Institute of Pathogen Biology, Chinese Academy of Medical Sciences and Peking Union Medical College, Beijing

Yan Liu
NHC Key laboratory of Systems Biology of Pathogens, Institute of Pathogen Biology, Chinese Academy of Medical Sciences and Peking Union Medical College, Beijing

Xiaobo Lei
NHC Key laboratory of Systems Biology of Pathogens, Institute of Pathogen Biology, Chinese Academy of Medical Sciences and Peking Union Medical College, Beijing

Pei Li
NHC Key laboratory of Systems Biology of Pathogens, Institute of Pathogen Biology, Chinese Academy of Medical Sciences and Peking Union Medical College, Beijing

Dan Mi
NHC Key laboratory of Systems Biology of Pathogens, Institute of Pathogen Biology, Chinese Academy of Medical Sciences and Peking Union Medical College, Beijing

Lili Ren
NHC Key laboratory of Systems Biology of Pathogens, Institute of Pathogen Biology, Chinese Academy of Medical Sciences and Peking Union Medical College, Beijing

Li Guo
NHC Key laboratory of Systems Biology of Pathogens, Institute of Pathogen Biology, Chinese Academy of Medical Sciences and Peking Union Medical College, Beijing

Ting Chen
NHC Key laboratory of Systems Biology of Pathogens, Institute of Pathogen Biology, Chinese Academy of Medical Sciences and Peking Union Medical College, Beijing

Jiaxing Hu
NHC Key laboratory of Systems Biology of Pathogens, Institute of Pathogen Biology,

Chinese Academy of Medical Sciences and Peking Union Medical College, Beijing

Zichun Xiang
NHC Key laboratory of Systems Biology of Pathogens, Institute of Pathogen Biology, Chinese Academy of Medical Sciences and Peking Union Medical College, Beijing

Zhixia Mu
NHC Key laboratory of Systems Biology of Pathogens, Institute of Pathogen Biology, Chinese Academy of Medical Sciences and Peking Union Medical College, Beijing

Xing Chen
Institute of Medicinal Plant Development (IMPLAD), Chinese Academy of Medical Sciences and Peking Union Medical College, Beijing

Jieyong Chen
Hengshui Third People's Hospital, Heibei

Keping Hu
Institute of Medicinal Plant Development (IMPLAD), Chinese Academy of Medical Sciences and Peking Union Medical College, Beijing

Qi Jin
NHC Key laboratory of Systems Biology of Pathogens, Institute of Pathogen Biology, Chinese Academy of Medical Sciences and Peking Union Medical College, Beijing

jinqi@ipbcams.ac.cn*Corresponding Author*

Jianwei Wang
NHC Key laboratory of Systems Biology of Pathogens, Institute of Pathogen Biology, Chinese Academy of Medical Sciences and Peking Union Medical College, Beijing

wangjw28@163.com*Corresponding Author*

Zhaohui Qian
NHC Key laboratory of Systems Biology of Pathogens, Institute of Pathogen Biology, Chinese Academy of Medical Sciences and Peking Union Medical College, Beijing

zqian2013@sina.com*Corresponding Author*

DOI:
10.21203/rs.2.24016/v1

SUBJECT AREAS
Virology *Molecular Biology*

KEYWORDS
Coronaviruses, 2019-nCoV, lentiviral based pseudovirus system, S protein, virus entry, hACE2, PIKfyve, TPC2, cathepsin L

Abstract

Since beginning of this century, there have already been three zoonotic outbreaks caused by beta coronaviruses (CoV), SARS-CoV in 2002-2003, MERS-CoV in 2012, and the newly identified 2019-nCoV in late 2019, Wuhan, China. As to Feb 10th, 2020, there are over 40,000 confirmed cases and over 900 deaths. However, little is known about the biology of this newly emerged virus. Here we developed a lentiviral based pseudovirus system for S protein of 2019-nCoV to study virus entry in BSL2 settings. First, we confirmed that human angiotensin converting enzyme 2 (hACE2) is the main entry receptor for 2019-nCoV. Second, we found that 2019-nCoV S protein mediated entry on 293/hACE2 cells was mainly through endocytosis, and PIKfyve, TPC2, and cathepsin L are critical for virus entry. Third, 2019-nCoV S protein is less stable than SARS-CoV, and it could trigger protease-independent and receptor dependent cell-cell fusion, which might help virus rapidly spread from cell to cell. Finally and more importantly, polyclonal anti-SARS S1 antibodies T62 effectively inhibited entry of SARS-CoV S pseudovirions, but almost had no effect on entry of 2019-nCoV S pseudovirions. Further studies using sera from one recovered SARS-CoV patient and five 2019-nCoV patients showed that there was only limited cross-neutralization activities between SARS-CoV and 2019-nCoV sera, suggesting that recovery from one infection might not protect against the other. Our results present potential targets for development of drugs and vaccines for 2019-nCoV.

Introduction

Coronaviruses (CoVs) infect human and animals and cause varieties of diseases, including respiratory, enteric, renal, and neurological diseases [1]. They are classified into four genera, alpha-CoV, beta-CoV, gamma-CoV, and delta-CoV [2]. Since beginning of this century, there have already been three zoonotic outbreaks of beta-CoVs. In 2002–2003,

severe acute respiratory syndrome coronavirus (SARS-CoV) [3,4], a lineage B beta-CoV, emerged from bat and palm civet [5,6], and infected over 8000 people and caused about 800 deaths [7]. In 2012, Middle East respiratory syndrome coronavirus (MERS-CoV), a lineage C beta-CoV, was discovered as the causative agent of a severe respiratory syndrome in Saudi Arabia [8], currently with 2494 confirmed cases and 858 deaths [9], it remains endemic in Middle East, and dromedary camel is considered as the zoonotic reservoir host of MERS-CoV. At the end of 2019, a novel coronavirus, tentatively named 2019-nCoV, was found in patients with severe pneumonia in Wuhan, China [10–12]. Viruses were isolated from patients and sequenced. Phylogenetical analysis revealed that it is a lineage B beta-CoV and closely related to a SARS-like CoV, RaGT13, discovered in a cave of Yunnan, China, in 2013 [13]. They share about 96% nucleotide sequence identities, suggesting that 2019-nCoV might emerge from a Bat SL-CoV. However, the intermediate host or whether there is an intermediate host remains to be determined.

CoV uses its spike glycoprotein (S), a main target for neutralization antibody, to bind its receptor, and mediate membrane fusion and virus entry. Each monomer of trimeric S protein is about 180 kDa, and contains two subunits, S1 and S2, mediating attachment and membrane fusion, respectively. In the structure, N- and C- terminal portions of S1 fold as two independent domains, N-terminal domain (NTD) and C-terminal domain (C-domain) (Fig 1A). Depending on the virus, either NTD or C-domain can serve as the receptor binding domain (RBD). While RBD of mouse hepatitis virus (MHV) is located at the NTD [14], most of other CoVs including SARS-CoV and MERS-CoV use C-domain to bind their receptors [15–19]. MHV uses mouse carcinoembryonic antigen related cell adhesion molecule 1a (mCEACAM1a) as the receptor [20], and the receptors for SARS-CoV and MERS-CoV are

human angiotensin-converting enzyme 2 (hACE2)[21] and human dipeptidyl peptidase 4 (hDPP4)[22], respectively. While S proteins of 2019-nCoV share overall higher percentage of amino acid identities with SL-CoV ZC45 [23] than SARS-CoV, the amino acid sequence of potential RBD of 2019-nCoV is more homologous to that of SARS-CoV (74%) than SL-CoV ZC45 (72%). Recently, Zhou et al reported that 2019-nCoV uses hACE2 as the receptor [13]. CoV S proteins are typical class I viral fusion proteins like influenza hemagglutinin (HA), protease cleavage in S2 is required for “priming” the fusion potential of S protein, activated by receptor binding. Depending on virus strains and cell types, CoV S proteins may be cleaved by one or several particular host proteases, including furin, trypsin, cathepsins, transmembrane protease serine protease–2(TMPRSS–2), TMPRSS–4, or human airway trypsin-like protease (HAT) [24–31]. Availability of these proteases on target cells largely determines whether CoVs enter cells through plasma membrane or endocytosis. However, whether any of these proteases could promote virus entry of 2019-nCoV remain elusive.

In this study, using a lentiviral pseudotype system, we determined cell type susceptibility, virus receptor, entry pathway, and protease priming for 2019-nCoV, and identified several potential drug targets for 2019-nCoV. Surprisingly, we also found that limited cross-neutralization between convalescent sera from SARS-CoV and 2019-nCoV patients.

Results

To enhance expression of the S protein of 2019-nCoV in mammalian cells, a codon-optimized cDNA encoding the S protein and 3xFLAG tag was synthesized, and to facilitate incorporation of S protein into lentiviral pseudovirons, the last 19 amino acids containing an ER-retention signal from the cytoplasmic tail of the S protein was removed (Fig 1A). The new construct was named 2019-nCoV S here. HEK 293T cells were transfected with

2019-nCoV S plasmid and expression of 2019-nCoV S protein was determined by western blot. There were two major bands, 180 kDa, and 90 kDa, detected by mouse anti-FLAG M2 antibody (Fig 1B, lane 2), reflecting the full length and cleaved S proteins, respectively. The band above 250 kDa likely results from dimeric or trimeric S proteins. Consistent with our previous report [27], MERS-CoV S protein was detected by polyclonal goat anti-MHV S antibodies AO4 (Fig 1C). Interestingly, both 2019-nCoV and SARS S proteins were also detected by polyclonal goat anti-MHV S antibodies AO4, suggesting the presence of a conserved immunogenic epitope among all four different CoVs, likely in S2. Surprisingly, although S1 subunits of 2019-nCoV and SARS-CoV share almost 64% in amino acid identities, 2019-nCoV S protein was barely detected by rabbit polyclonal anti-SARS S1 antibodies T62 (Fig 1D), suggesting that the major epitope(s) for T62 antibodies should lie in the region of S1 where the sequence differs between SARS-CoV and 2019-nCoV. The 2019-nCoV S protein was not detected by either the monoclonal anti-SARS S1 antibody or anti-MERS S2 antibody.

The efficiency of 2019-nCoV S protein incorporation into pseudovirions was also evaluated using monoclonal mouse anti-FLAG M2 antibody and polyclonal goat anti-MHV S antibody AO4. While majority of SARS-CoV S proteins incorporated into pseudovirons were full length, at 180 kDa (Fig 1H and 1I), most of 2019-nCoV S proteins on lentiviral pseudovirions were cleaved, about 90 kDa (Fig 1G and 1H), likely reflecting presence of extra furin site (R682-R683-A684-R685, Fig 1A) between S1 and S2 in 2019-nCoV S protein. Consistent with the results in cell lysate (Fig 1D), SARS-CoV S proteins, but not 2019-nCoV S proteins, in pseudovirions was readily detected by using polyclonal rabbit anti-SARS S1 antibodies T62 (Fig 1I).

Next, we determined whether 2019-nCoV S pseudovirions were able to transduce human, monkey, and bat cells. VSV-G pseudovirons were used as a positive control, whereas bald

particles with no spike proteins (mock) were served as a negative control. As expected, all cell types were effectively transduced by VSV-G pseudovirons (Fig 2A). Compared to mock control, 2019-nCoV S pseudovirions showed an over 500-fold increase in luciferase activities in Calu3 cells, at a level similar to SARS-CoV S pseudovirions (Fig 2A). Huh7 and Vero 81 cells also gave about 10-fold increase in luciferase activities when transduced by 2019-nCoV. Interestingly, while LLCMK2 cells were highly transduced by SARS-CoV S pseudovirions, it only showed very limited transduction by 2019-nCoV S pseudovirions (Fig 2A), suggesting that there might be some differences on virus entry on LLCMK2 cells mediated by S proteins between 2019-nCoV and SARS-CoV. We then investigated whether any known CoV receptors might be used by 2019-nCoV S protein as entry receptor. The 2019-nCoV S pseudovirons were used to transduce BHK cells stably expressing human aminopeptidase N (hAPN), the receptor for human CoV 229E, 293 cells stably expressing hACE2 (293/hACE2), the receptor for SARS-CoV, and HeLa cells stably expressing hDPP4 (HeLa/hDPP4), the receptor for MERS-CoV. While BHK/hAPN and HeLa/hDPP4 cells were not susceptible for the transduction of 2019-nCoV S pseudovirions, 293/hACE2 cells were highly transduced by 2019-nCoV S pseudovirions, indicating that hACE2 might be the receptor for 2019-nCoV. We then determined whether 2019-nCoV S protein could directly bind to hACE2 protein. HEK 293T cells transiently expressing 2019-nCoV S protein were incubated with soluble hACE2 and analyzed by flow cytometry. As shown in Fig 2C, 2019-nCoV S protein bound to soluble hACE2 at a level similar to SARS-CoV S protein, although the mean fluorescence intensity (MFI) for 2019-nCoV S protein was slightly lower than SARS-CoV S protein. To further investigate if hACE2 is the receptor for 2019-nCoV, we performed inhibition experiments using soluble hACE2. Soluble hACE2 proteins were pre-incubated with 2019-nCoV S pseudovirons on ice for 1 hr, then virus-protein mixture was added onto 293/hACE2 cells. Entry of 2019-nCoV S pseudovirions was significantly

prevented by pre-incubation of soluble hACE2 at both 10 g/ml and 50 g/ml (Fig 2D), further supporting the notion that hACE2 is the receptor.

Since majority of S proteins on 2019-nCoV S pseudovirions are cleaved, we then determined whether 2019-nCoV S pseudovirons entered cells through endocytosis or cell surface. HEK 293/hACE2 cells were treated with lysosomotropic agents, ammonia chloride and bafilomycin A, and their effect on virus entry was evaluated. Consistent with previous reports, 20 mM NH_4Cl and 100 nM bafilomycin A decreased entry of SARS-CoV S and VSV-G pseudovirions by over 99%, compared to no treatment control. More than 98% reduction in transduction on 293/hACE2 cells by 2019-nCoV S pseudovirions was also shown when the cells were incubated with either NH_4Cl or bafilomycin A (Fig 3A), indicating that 2019-nCoV S pseudovirions enter 293/hACE2 cells mainly though endocytosis, despite that its spike proteins were cleaved.

Phosphoinositides play many essential roles in endocytosis. Among them, one is phosphatidylinositol–3,5-bisphosphate ($PI(3,5)P_2$), which regulates early endosome to late endosome dynamics [32,33]. Phosphatidylinositol–3-phosphate 5-kinase (PIKfyve) is the main enzyme synthesizing $PI(3,5)P_2$ in early endosome. HEK 293/hACE2 cells were treated with apilimod, a potent inhibitor for PIKfyve [34]. Inhibition of PIKfyve by apilimod significantly reduced entry of SARS-CoV S pseudovirions on 293/hACE2 cells in a dose dependent manner (Fig 3B), whereas it had no effect on entry of VSV-G pseudovirions, which occurred in early endosome. Similar inhibitory effects were observed when HeLa/hDPP4 cells and HeLa cells stably expressing mouse carcinoembryonic antigen related cell adhesion molecule 1a (mCEACAM1a) (HeLa/mCEACAM1a) were treated with apilimod and transduced with MERS-CoV and MHV S pseudovirions (Fig 3B), respectively. Moreover, infection of live MHV on 17Cl.1 cells was also strongly inhibited by apilmod treatment (Fig 3C), no

significant cell toxicity was observed on apilimod at any concentration tested (Fig 3C). We then determined whether apilimod could inhibit entry of 2019-nCoV S pseudovirions on 293/hACE2. As expected, apilimod treatment significantly inhibited entry of 2019-nCoV S pseudovirions in a dose dependent manner (Fig 3D). Similar effects were shown when 293/hACE2 cells were treated with YM201636, another PIKfyve inhibitor (Fig 3E). These results suggested that PIKfyve might be a potential general drug target for viruses that enter cells through endocytosis. Two pore channel subtype 2 (TPC2) and TRPML1 in lysosome are two major downstream effectors of $PI(3,5)P_2$ [35]. While blocking TPC2 activity by tetrandrine, a inhibitor for TPC2 [36], significantly decreased entry of 2019-nCoV S pseudovirions (Fig 3F), treatment of cells with 130, a TRPML1 inhibitor, had no effect (Fig S1), indicating that TPC2, not TRPML1, is important for 2019-nCoV entry.

Protease “priming” on S protein is an important step for coronavirus entry, and cathepsins in lysosome have been shown to be critical for SARS-CoV and MERS-CoV entry through endocytosis. To investigate whether cathepsins are required for 2019-nCoV entry. HEK 293/hACE2 cells were treated with either a broad inhibitor for cathepsin B, H, L, and calpain (E64D), cathepsin L inhibitor (SID 26681509), or cathepsin B inhibitor (CA–074). VSV-G pseudovirions were used as a negative control, since virus entry mediated by VSV-G does not require protease activation. E64D treatment of 293/hACE2 cells reduced entry of 2019-nCoV S pseudovirions by 92.5%, indicating that at least one of cathepsins or calpain might be required for 2019-nCoV entry (Fig 4A). While cathepsin B inhibitor treatment did not showed any marked effect on virus entry, cathepsin L inhibition treatment decreased entry of 2019-nCoV S pseudovirions into 293/hACE2 by over 76% (Fig 4A), suggesting that cathepsin L should be essential for priming of 2019-nCoV S protein in lysosome for entry into 293/hACE2 cells.

Trypsin cleavage can also activate the fusion potential of SARS-CoV and MERS-CoV S protein and induce receptor-dependent syncytium formation. We then tested whether 2019-nCoV S protein cleaved by trypsin could trigger syncytia on 293/hACE2 cells. HEK 293T cells expressing 2019-nCoV S proteins were overlaid on 293/hACE2 cells in either presence or absence of trypsin. Consistent to our previous report, addition of trypsin triggered massive syncytium formation on 293/hACE2 cells by SARS-CoV S protein after 4 hrs incubation (Fig 4B and 4C). Large syncytia were also formed at a level similar to SARS-CoV S proteins when 2019-nCoV S protein expressing 293T cells were added onto 293/hACE2 cells with trypsin. Of note, 2019-nCoV, not SARS-CoV, S proteins also induced significantly amount of syncytia on 293/hACE2 cells even in the absence of trypsin (Fig 4C), suggesting that 2019-nCoV S proteins could be triggered upon the receptor binding without additional protease “priming”. We then investigated whether 2019-nCoV S protein was less stable and easier to be triggered than SARS-CoV S protein by comparing their thermostability. An A82V mutation in glycoprotein (gp) of Ebola virus with lower thermostability has been linked to 2013–2016 Ebola virus outbreak [37–39]. Compared to SARS-CoV S protein, 2019-nCoV S protein was clearly less stable, requiring significant shorter time and lower temperature to be inactivated (Fig 4D and 4E), suggesting that 2019-nCoV S protein might be easier to be triggered. We also found that expressing type II membrane serine protease (TMPRSS) 2, 4, 11A, 11D, and 11E on 293/hACE2 cells significantly enhance 2019-nCoV S protein mediated cell-cell fusion (Fig S2).

Since 2019-nCoV S reacted weakly with polyclonal rabbit anti-SARS S1 antibodies T62 in western blot, we then investigated whether 2019-nCoV S protein in native conformation could be recognized by anti-SARS S1 antibodies T62. HEK 293T cells transiently expressing 2019-nCoV S proteins were incubated with polyclonal anti-SARS S1 antibodies T62 and analyzed by flow cytometry. SARS-CoV S was used as a positive control. As expected,

expression of SARS-CoV S proteins on 293T cell surface were readily detected by polyclonal anti-SARS S1 antibodies T62 (Fig 5A). On the contrast, only low level of binding of 2019-nCoV S protein to polyclonal rabbit anti-SARS S1 antibodies T62 was detected (Fig 5A), further indicating that there might be limited cross-reacting activities against 2019-nCoV S protein in polyclonal rabbit anti-SARS S1 antibodies T62. To further delineate where the epitopes for this polyclonal antibodies are located, two new constructs were generated, a SARS-CoV S protein backbone with RBD from 2019-nCoV (SARS-CoV S/nRBD) and a 2019-nCoV S protein backbone with RBD from SARS-CoV (2019-nCoV S/sRBD). Replacement of SARS-CoV RBD with 2019-nCoV RBD (SARS-CoV S/nRBD) dramatically decreased binding of polyclonal antibodies T62 to S protein, whereas substitution of 2019-nCoV RBD with SARS-CoV RBD (2019-nCoV S/sRBD) greatly increased the affinity of S protein to polyclonal antibodies T62 (Fig 5A). All chimera proteins were expressed at levels similar to 2019-nCoV S protein (Fig 5B, top panel). These results suggest that at least one major epitope for polyclonal antibodies T62 might be located in RBD where the sequences differ between SARS-CoV and 2019-nCoV (Fig 5C). Of note, while 2019-nCoV S/sRBD bound to polyclonal antibodies T62 much better than SARS-CoV S/nRBD in flow cytometry, the signal for SARS-CoV S/nRBD was much stronger than 2019-nCoV S/sRBD in western blot by polyclonal antibodies T62. Among residues in SARS-CoV RBD critical for receptor binding and virus entry [40,41], seven of them are different between SARS-CoV and 2019-nCoV RBDs (Fig 5C). We then mutated each of them in SARS-CoV S protein to the corresponding residues in 2019-nCoV S. None of any mutants except for Y442L substitution had major effect on SARS-CoV S protein expression (Fig S3) and binding of SARS-CoV S to polyclonal rabbit anti-SARS S1 antibodies T62 (Fig 5D), suggesting that any of these residues might not be any direct antigenic sites for polyclonal antibodies T62. Next, we tested whether polyclonal rabbit anti-SARS S1 antibodies T62 could inhibit entry

of 2019-nCoV S pseudovirions. CoV S protein pseudovirions were incubated with polyclonal antibodies T62 on ice for 1 hr, and their transduction was measured according to luciferase activities. As expected, polyclonal antibodies T62 neutralized SARS-CoV S pseudovirion effectively in a dose dependent manner (Fig 5E). In contrast, even at a concentration of 50 g/ml, polyclonal antibodies T62 did not have marked effect on transduction by 2019-nCoV S proteins (Fig 5E).

Because rabbit polyclonal anti-SARS S1 antibodies did not show significant neutralization activity against 2019-nCoV S pseudovirions, we then asked whether sera from recovered SARS-CoV and 2019-nCoV patients could neutralize SARS-CoV S and 2019-nCoV S pseudovirions. We obtained sera from one recovered SARS-CoV patient and five recovered 2019-nCoV patients and tested their neutralization activities against transduction on 293/hACE2 cells by SARS-CoV and 2019-nCoV S pseudovirions. Serum from recovered SARS-CoV patient showed strong inhibition on transduction by SARS-CoV S pseudovirions, and it had modest neutralization activity against 2019-nCoV S pseudovirons (Fig 6A and Table 1). In contrast, sera from all five 2019-nCoV patients neutralized 2019-nCoV S pseudovirions effectively, and none of them had any effect on transduction by SARS-CoV S pseudovirions (Fig 6B and Table 1).

Discussion

About 70% of the emerging pathogens infecting humans originate from animals, and CoVs are among the forefronts of these pathogens [42]. The newly emerged 2019-nCoV infects human and causes severe pneumonia, and as Feb 10th, 2020, current outbreak has spread to 25 countries with total over 40000 confirmed cases and 900 deaths [43]. However, little is known about its biology. Since the virus is categorized as a biosafety level 3 (BSL3) agent, according to WHO guideline, we developed a pseudotype system with S protein of

2019-nCoV to study virus entry in BSL2 settings. Understanding how 2019-nCoV enters cell will provide valuable information for virus pathogenesis, vaccine design, and drug target. Utilizing this pseudotype system, we screened a panel of human and monkey cells line for their susceptibility of 2019-nCoV S mediated transduction. It is not a surprise that we found that human lung cancer cell line Calu3 is highly susceptible, since 2019-nCoV is, ultimately, a human respiratory virus causing pneumonia. However, it is a surprise that LLCMK2 cells, a resus monkey kidney epithelium cell line, were highly susceptible to SARS-CoV S transduction, but only showed limited transduction by 2019-nCoV S pseudovirions. Both S proteins use hACE2 as the receptor for binding and entry, which we further confirmed by flow cytometry analysis and competitive inhibition experiment using soluble hACE2 in this study (Fig 3B and 3C). While full length S proteins of 2019-nCoV and SARS-CoV S share almost 76% identities in amino acid sequences, there are only 53.5% homology in their NTDs. Of note, NTDs of different CoVs S proteins have been shown to bind different sugar etc. While NTD of MERS-CoV prefers α2,3-linked sialic acid over α2,6-linked sialic acid [44], NTDs of human CoVs OC43 and HKU1 bind to 9-O-acetylated sialic acids [45,46]. No sugar binding has been reported for NTD of SARS-CoV. Whether NTD of 2019-nCoV binds to sugar and effect of sugar binding of NTD on virus entry remains to be determined.

Successful conformational changes of S proteins leading to membrane fusion not only require receptor binding, but also need appropriate protease cleavage to release restrain of fusion peptide. There is a furin site between S1 and S2 (amino acids 682–685, RRAR) subunits in 2019-nCoV S protein, and it renders cleavage of S protein to S1 and S2 during transportation from ER to plasma membrane, similar to what happens in high pathogenic influenza viruses. Whether the presence of this furin site has any effect on viral

pathogenesis and virus spreading among humans remains to be determined. Although majority of 2019-nCoV S proteins in pseuodvirions were cleaved, endocytosis remains to be its main entry pathway on 293/hACE2 cell. Lysosomal cathepsin L, not B, appears to be critical for 2019-nCoV S protein activation, inhibition of cathepsin L activity by specific drug effectively reduced virus entry, similar to what reported in SARS-CoV and MERS-CoV [26,27,47]. Trypsin could also activate 2019-nCoV S protein efficiently and induce large syncytium formation. Surprisingly, we found that, even without trypsin, 2019-nCoV S protein could trigger significant amount of syncytium formation on 293/hACE2 cells, a phenomena similar to what observed in MHV S protein in certain aspect [48]. This led us to speculate that 2019-nCoV S protein capable of triggering protease-independent and receptor-dependent syncytium formation might enhance virus spreading through cell-cell fusion and this might partially explain rapid progress of the diseases [10,11].

Recently studies showed that early to late endosome maturation is regulated by $PI(3,5)P_2$, and inhibition of PIKfyve, the key enzyme synthesizing $PI(3,5)P_2$, and TPC2, a downstream effector in lysosome, significantly reduced virus entry of MERS-CoV [49]. We also confirmed this in this study, and further showed that blocking PIKfyve and TPC2 also strongly inhibited entry mediated by 2019-nCoV S protein, indicating that $PI(3,5)P_2$ pathway might be considered as potential general drug targets for CoV infection.

CoV S protein is one of key component determining virus virulent, tissue tropism, host range and is also one of main targets for neutralization antibodies and vaccine design. Although the S proteins of 2019-nCoV and SARS-CoV are highly homologous, to our surprise, polyclonal rabbit anti-SARS S1 antibodies T62 did not bind to 2019-nCoV S protein well, and poorly neutralized 2019-nCoV S protein mediated virus entry. Further analysis reveals that major immune-epitopes for T62 antibodies likely lie in the region of

RBD (Fig 4A), particularly where the amino acid sequences differ between 2019-nCoV and SARS-CoV. The findings that there was lack of neutralization activity for 2019-nCoV entry by T62 antibodies led us hypothesize that convalescent sera from recovered SARS –CoV infected patients may only provide minimal protection against 2019-nCoV infection, and *vice versa.* As expected, there were lack of cross-neutralization activities between 2019-nCoV and SARS-CoV convalescent sera, suggesting that those previously recovered from SARS-CoV infection may not be fully protected against 2019-nCoV infection, and *vis versa.* In conclusion, we demonstrated that 2019-nCoV S protein mediated entry on 293/hACE2 cells mainly through endocytosis, and PIKfyve, TPC2, and cathepsin L are critical for virus entry. We further found that 2019-nCoV S protein could trigger protease-independent syncytia and there was limited cross-neutralization activities of sera between SARS-CoV and 2019-nCoV patients. Our findings will provide potential targets for development of drugs and vaccines against this newly emerging lineage B beta-CoV.

Materials And Methods

Constructs and plasmids

Codon-optimized cDNA encoding 2019-nCoV S glycoprotein with C-terminal 19 amino acids deletion was synthesized and cloned into eukaryotic cell expression vector pCMV14–3×Flag between the *Hind* III and *BamH* I sites. Plasmids encoding SARS-CoV S glycoprotein, MERS-CoV S glycoprotein and MHV S glycoprotein were constructed as previously described [50]. The VSV-G encoding plasmid and lentiviral packaging plasmid psPAX2 were obtained from Addgene (Cambridge, MA). The pLenti-GFP lentiviral reporter plasmid that expresses GFP and luciferase was generously gifted by Fang Li, Duke University.

Cell lines

Human embryonic kidney cell line 293 and 293T containing the SV40 T-antigen, human

airway epithelial cell line Calu 3, human alveolar epithelial cell line A549, human fibroblasts derived from lung tissue MRC5, human carcinoma cell line derived from hepatocyte Huh7, African green monkey kidney cell line Vero E6 and Vero 81, human cervical carcinoma cell line HeLa, were obtained from ATCC (Manassas, VA, USA). Bat embryo fibroblast cells RS were isolated mid-gestation fetuses from *Rhinolophus sinicus* bat. HEK 239 cells stably expressing recombinant human ACE2 (293/hACE2), baby hamster kidney fibroblasts stably expressing recombinant human APN (BHK/hAPN), HeLa cells stably expressing recombinant human DPP4 (HeLa/hDPP4) were established in our lab by overexpression of these receptors. All above cells were maintained in Dulbecco's MEM containing 10% fetal bovine serum and 100 unit penicillin, 100µg streptomycin, and 0.25µg Fungizone (1% PSF, Gibco) per milliliter. Rhesus monkeys kidney cell line LLC-MK2 from ATCC was maintained in Opit-MEM containing 10% FBS and 1%PSF.

Antibodies and inhibitors

Broad-spectrum cysteine protease inhibitor E64D (#HY–100229), Cathepsin B specific inhibitor SID 26681509 (#HY–103353), cathepsin B specific inhibitor CA–074 (#HY–103350), PIKfyve inhibitors apilimod (#HY–14644) and YM201636 (#HY–13228), were purchased from Med Chem Express (MCE, New Jersey, USA). Calcium channel blocker tetrandrine (#S2403) was purchased from Selleck Chemicals (Texas, USA). Endosome acidification inhibitors NH_4Cl (#A9434) and bafilomycin A (#19–148) were purchased from Sigma-Aldrich (St. Louis, MO, USA). Rabbit polyclonal against SARS S1 antibodies (#40150-T62), mouse monoclonal against MERS-CoV S2 antibody (#40070-MM11), mouse monoclonal against SARS S1 antibody (#40150-MM02), rabbit polyclonal against HIV–1 Gag-p24 antibody (11695-RB01) were purchased from Sino Biological Inc. (Beijing, China). Goat polyclonal against human ACE2 antibody (#AF933) was purchased from R&D Systems

(Minnesota, USA). Mouse monoclonal anti-FLAG M2 antibody was purchased from Sigma-Aldrich. Donkey Anti-Rabbit IgG (#711–035–152), Goat Anti-Mouse IgG (#115–035–146), Rabbit Anti-Goat IgG (#305–035–003) were purchased from Jackson ImmunoResearch (West Grove, PA, USA). Alexa Fluor 488-conjugated goat anti-rabbit IgG, Alexa Fluor 488-conjugated goat anti-mouse IgG were purchased from ZSGB-Bio LLC (Beijing, China).

Production of 2019-nCoV pseudovirions and spike-mediated virus entry

Pseudovirions were produced by co-transfection 293T cells with psPAX2, pLenti-GFP, and plasmids encoding either 2019-nCoV S, SARS-CoV S, VSV-G, or empty vector by using polyetherimide (PEI). The supernatants were harvested at 40, 64 hrs post transfection, passed through 0.45 m filter, and centrifuged at 800g for 5 minutes to remove cell debris. To transduce cells with pseudovirions, cells were seeded into 24-well plates and inoculated with 500µl media containing pseudovirions. After overnight incubation, cells were fed with fresh media. About 40 hrs post-inoculation, cells were lysed with 120 l medium containing 50% Steady-glo (promega) at room temperature for 5 minutes. The transduction efficiency was measured by quantification of the luciferase activity using a Modulus II microplate reader (Turner Biosystems, Sunnyvale, CA, USA). All experiments were done in triplicates, and repeated at least twice or more.

Detection of spike glycoprotein of 2019-nCoV by western blot.

The spike glycoprotein of 2019-nCoV in cells and on pseudovirions were detected by using western blot as previously described [51]. Briefly, cells transfected with plasmids encoding spike glycoprotein of 2019-nCoV, SARS-CoV, MERS-CoV, and MHV were lysed at 40 hrs post transfection by RIPA buffer (20mM Tris-HCl pH 7.5, 150mM NaCl, 1mM EDTA, 0.1% SDS, 1% NP40, 1×protease inhibitor cocktail). To pellet down pseudovirions, the viral supernatants were centrifuged at 25000 rpm for 2 hrs in a Beckman SW41 rotor at 4℃ through a 20%

sucrose cushion, and virus pellets were resuspended into 30 l RIPA buffer. The samples were boiled for 10 minutes and separated in a 10% SDS-PAGE gel and transferred to nitrocellulose filter membranes. After blocked by 5% milk, the membranes were blotted with primary antibodies, followed by incubated with horseradish peroxidase (HRP) conjugated secondary antibodies and visualized with Chemiluminescent Reagent (Bio-Rad). MHV S proteins were detected using polyclonal goat anti-MHV S antibody AO4 (1:2,000); SARS-CoV S proteins were blotted with either polyclonal anti-SARS S1 antibodies T62 (1:2,000) (Sinobiological Inc, Beijing, China) or mouse monoclonal against SARS S1 antibody MM02 (1:1,000) (Sinobiological Inc, Beijing, China), MERS-CoV and 2019-nCoV S proteins were detected using mouse monoclonal anti-MERS S (1:1,000) (Sinobiological Inc, Beijing, China) and anti-FLAG M2 antibody (1:1,000)(Sigma, St Louis, MO, USA), respectively.

Effects of lysosomotropic agents and cathepsin inhibitors on psuedovirion entry

HEK 293/hACE2 cells were pretreated with either lysosomotropic agents (endosome acidification inhibitor NH_4Cl and bafilomycin A; PIKfyve inhibitor apilimod and YM201636; calcium channel blocker tetrandrine) or cathepsin inhibitors (cathepsin L inhibitor SID26881509, cathepsin B inhibitor CA–074, and cathepsin inhibitor E64D) for 1 hr at 37℃, then spin-inoculated with psuedovirions in the presence of inhibitor at 1200g for 30 minutes. After overnight incubation, cells were fed with fresh medium without inhibitor. Cells were lysed at 48 hrs post inoculation and their luciferase activity was measured.

Flow cytometric analysis of S protein expression

Briefly, 293T cells were transfected with 2 μg of plasmids encoding either 2019-nCoV S, SARS-CoV S or MERS-CoV S protein using PEI. Forty hours later, cells were detached by

using PBS with 1 mM EDTA. After washing, cells were incubated with polyclonal rabbit anti-SARS S1 antibodies T62 (1:200 dilution) (Sinobiological Inc., Beijing, China) for 1 hr on ice, followed by Alexa Fluor 488-conjugated goat anti-rabbit IgG (1:200) (ZSGB-Bio LLC, Beijing, China) for 1h. Cells were then analyzed by flow cytometry.

MTT assay

MTT assay was used to assess cell viability. Briefly, cells were seeded into a 96-well plate at a cell density of 3,000 per well and allowed to adhere for 24 h, followed by treatment with serially diluted inhibitors for 12 h. 2 μl of 5 mg/mL MTT was added to the medium 24 h later and incubated for 4 h at 37˚C. After removing the culture medium, 100 μl of DMSO was added. The absorbance was measured at 570nm using a microplate spectrophotometer (Multiskan FC, Thermo Scientific). All experiments were performed in triplicate, and the cell viability of cells was calculated as the ratio of each experimental condition to the control.

Cell-cell fusion assay

Cell-cell fusion assays were performed as previously described with minor modifications [50]. Briefly, HEK–293T cells were co-transfected with plasmids encoding CoV S glycoprotein and eGFP. For trypsin-dependent cell-cell fusion, cells were detached with trypsin (0.25%) at 40 hrs post-transfection and overlaid on an 80% confluent monolayer of 293/hACE2 cells at a ratio of approximately one S-expressing cell to three receptor-expressing cells. For trypsin-independent cell-cell fusion, cells were detached with 1 mM EDTA and overlaid on 293/hACE2 cells. After 4 hrs incubation, images of syncytia were captured with a Nikon TE2000 epifluorescence microscope running MetaMorph software (Molecular Devices). All experiments were done in triplicate and repeated at least three times.

Construction, expression and purification of soluble human ACE2.

Construction, expression and purification of soluble human ACE2 were performed as previously described with minor modifications [50]. Briefly, DNA fragments encoding residues 19–615 of human hACE2 with N-terminal FLAG and 6×his tags were cloned between Sal I and Hind III of modified pFASTBac1 vector with gp67 signal peptide. The soluble receptors were expressed in High Five insect cells using the bac-to-bac system (Invitrogen) and purified using nickel affinity and ion-exchange chromatography.

Soluble hACE2 binding assay

HEK–293T cells were transfected with plasmids encoding 2019-nCoV S, SARS-CoV S or MERS-CoV S protein. Cells were detached with 1 mM EDTA 40 hrs post- transfection, washed twice with 3% FBS in 1×PBS, and incubated with 5 μg/mL soluble hACE2 for 1 hr on ice. After washing three times with 3% FBS in 1×PBS, cells were incubated with polyclonal goat anti-human ACE2 antibody (R&D Systems, MN, USA) for 1 hr, followed by FITC-conjugated rabbit anti-goat secondary antibody (Jackson ImmunoResearch, PA, USA). After washing, cells were then analyzed by flow cytometry.

Soluble hACE2 inhibition assay

Briefly, lentiviruses pseudotyped with 2019-nCoV S, SARS-CoV S or VSV-G were pre-incubated with serially diluted soluble hACE2 for 1 hr on ice. The mixture were then added on 293/hACE2 cells, followed by centrifugation inoculation for 1 hr at room temperature. Cells were fed with fresh medium 6 hrs later and lysed at 48 hrs post-inoculation. Pseudoviral transduction was measured according to luciferase activities.

Pseudovirus neutralization assay

SARS-CoV S, 2019-nCoV S, and VSV-G pseudovirions were pre-incubated with serially diluted either polyclonal rabbit anti-SARS S1 antibodies T62 or patient sera for 1 hr on ice, then virus-antibody mixture was added onto 293/hACE2 cells in a 96-well plate. After 6 hrs

incubation, the inoculum was replaced with fresh medium. Cells were lysed 40 hrs later and pseudovirus transduction was measured as previously described. Prior to experiments, patient sera were incubated at 56℃ for 30 mins to inactivate complement.

Serum collection

Five patients were hospitalized with pneumonia in Hengshui Third People's Hospital, Hengshui, Heibei province, China, and their respiratory specimens were collected for coronavirus detection and were positive for 2019-nCoV. After all patients recovered, their sera were collected with informed consent. Serum from a recovered SARS patient was also collected with informed consent.

Declarations

ACKNOWLEDGEMENT.

This work was supported by grants from Chinese Science and Technology Key Projects (2020YFC0841000 to ZQ), National Natural Science Foundation of China (31670164 and 31970171 to ZQ, and 81930063 to JW), and the CAMS Innovation Fund for Medical Sciences (2016–12M–1–014 to JW)

AUTHOR CONTRIBUTIONS

Z. Q. and J. W. conceived the projects, Z. Q., J. W., and J. Q. coordinated the projects. Z. Q. and J. W. designed the experiments with the help of X. O., Y. L., X. L., L. R., L. G., and J. Q. X. O., Y. L., X. L., P. L., D. M., R. G., T. C., and J. H. performed all the experiments. Z. Q. and J. W. analyzed the data with help of X. O., Y. L., X. L., L. R., and L. G. Z. Q. and J. W. wrote the manuscript with help of other authors.

References

1 Masters, P. S. & Perlman, S. in *Fields Virology* Vol. 1 (eds D.M. Knipe & P.M Howley) Ch. 28, 825-858 (2013).

2 Viruses, I. C. o. T. o. Virus Taxonomy: 2011 Release. http://ictvonline.org/virusTaxonomy.asp?version=2011. (2011).

3 Drosten, C. *et al.* Identification of a novel coronavirus in patients with severe acute respiratory syndrome. *N Engl J Med* **348**, 1967-1976, doi:10.1056/NEJMoa030747 NEJMoa030747 [pii] (2003).

4 Ksiazek, T. G. *et al.* A novel coronavirus associated with severe acute respiratory syndrome. *N Engl J Med* **348**, 1953-1966, doi:10.1056/NEJMoa030781 NEJMoa030781 [pii] (2003).

5 Guan, Y. *et al.* Isolation and characterization of viruses related to the SARS coronavirus from animals in southern China. *Science* **302**, 276-278, doi:10.1126/science.1087139 1087139 [pii] (2003).

6 Li, W. *et al.* Bats are natural reservoirs of SARS-like coronaviruses. *Science* **310**, 676-679, doi:1118391 [pii] 10.1126/science.1118391 (2005).

7 Kamps, B. S. & Hoffmann, C. *SARS Reference, http://www.sarsreference.com/sarsref/preface.htm*. (2003).

8 Zaki, A. M., van Boheemen, S., Bestebroer, T. M., Osterhaus, A. D. & Fouchier, R. A. Isolation of a novel coronavirus from a man with pneumonia in Saudi Arabia. *N Engl J Med* **367**, 1814-1820, doi:10.1056/NEJMoa1211721 (2012).

9 WHO. Middle East respiratory syndrome coronavirus (MERS-CoV) - update, World Health Organization Global Alert and Response, Nov, 2019 https://www.who.int/emergencies/mers-cov/en/. (2019).

10 Huang, C. *et al.* Clinical features of patients infected with 2019 novel coronavirus in Wuhan, China. *Lancet*, doi:10.1016/S0140-6736(20)30183-5 (2020).

11 Ren, L. L. *et al.* Identification of a novel coronavirus causing severe pneumonia in human: a descriptive study. *Chin Med J (Engl)*, doi:10.1097/CM9.0000000000000722 (2020).

12 Zhu, N. *et al.* A Novel Coronavirus from Patients with Pneumonia in China, 2019. *N Engl J Med*, doi:10.1056/NEJMoa2001017 (2020).

13 Zhou, P. *et al.* A pneumonia outbreak associated with a new coronavirus of probable bat origin. *Nature*, doi:10.1038/s41586-020-2012-7 (2020).

14 Kubo, H., Yamada, Y. K. & Taguchi, F. Localization of neutralizing epitopes and the receptor-binding site within the amino-terminal 330 amino acids of the murine coronavirus spike protein. *J Virol* **68**, 5403-5410 (1994).

15 Li, F., Li, W., Farzan, M. & Harrison, S. C. Structure of SARS coronavirus spike receptor-binding domain complexed with receptor. *Science* **309**, 1864-1868, doi:309/5742/1864 [pii] 10.1126/science.1116480 (2005).

16 Lu, G. *et al.* Molecular basis of binding between novel human coronavirus MERS-CoV and its receptor CD26. *Nature* **500**, 227-231, doi:nature12328 [pii] 10.1038/nature12328 (2013).

17 Wang, N. *et al.* Structure of MERS-CoV spike receptor-binding domain complexed with human receptor DPP4. *Cell Res* **23**, 986-993, doi:cr201392 [pii] 10.1038/cr.2013.92 (2013).

18 Ou, X. *et al.* Crystal structure of the receptor binding domain of the spike glycoprotein of human betacoronavirus HKU1. *Nature communications* **8**, 15216, doi:10.1038/ncomms15216 (2017).

19 Qian, Z. *et al.* Identification of the Receptor-Binding Domain of the Spike Glycoprotein of Human Betacoronavirus HKU1. *J Virol* **89**, 8816-8827,

doi:10.1128/JVI.03737-14 (2015).

20 Williams, R. K., Jiang, G. S. & Holmes, K. V. Receptor for mouse hepatitis virus is a member of the carcinoembryonic antigen family of glycoproteins. *Proc Natl Acad Sci U S A* **88**, 5533-5536 (1991).

21 Li, W. *et al.* Angiotensin-converting enzyme 2 is a functional receptor for the SARS coronavirus. *Nature* **426**, 450-454, doi:10.1038/nature02145 nature02145 [pii] (2003).

22 Raj, V. S. *et al.* Dipeptidyl peptidase 4 is a functional receptor for the emerging human coronavirus-EMC. *Nature* **495**, 251-254, doi:nature12005 [pii] 10.1038/nature12005 (2013).

23 Hu, D. *et al.* Genomic characterization and infectivity of a novel SARS-like coronavirus in Chinese bats. *Emerg Microbes Infect* **7**, 154, doi:10.1038/s41426-018-0155-5 (2018).

24 Bertram, S. *et al.* TMPRSS2 activates the human coronavirus 229E for cathepsin-independent host cell entry and is expressed in viral target cells in the respiratory epithelium. *J Virol* **87**, 6150-6160, doi:JVI.03372-12 [pii] 10.1128/JVI.03372-12 (2013).

25 Bertram, S. *et al.* Cleavage and activation of the severe acute respiratory syndrome coronavirus spike protein by human airway trypsin-like protease. *J Virol* **85**, 13363-13372, doi:10.1128/JVI.05300-11 (2011).

26 Gierer, S. *et al.* The Spike Protein of the Emerging Betacoronavirus EMC Uses a Novel Coronavirus Receptor for Entry, Can Be Activated by TMPRSS2, and Is Targeted by Neutralizing Antibodies. *J Virol* **87**, 5502-5511, doi:JVI.00128-13 [pii] 10.1128/JVI.00128-13 (2013).

27 Qian, Z., Dominguez, S. R. & Holmes, K. V. Role of the spike glycoprotein of

human Middle East respiratory syndrome coronavirus (MERS-CoV) in virus entry and syncytia formation. *PLoS One* **8**, e76469, doi:10.1371/journal.pone.0076469 PONE-D-13-26136 [pii] (2013).

28 Shirato, K., Kawase, M. & Matsuyama, S. Middle East respiratory syndrome coronavirus infection mediated by the transmembrane serine protease TMPRSS2. *J Virol* **87**, 12552-12561, doi:JVI.01890-13 [pii]10.1128/JVI.01890-13 (2013).

29 Shirogane, Y. *et al.* Efficient multiplication of human metapneumovirus in Vero cells expressing the transmembrane serine protease TMPRSS2. *J Virol* **82**, 8942-8946, doi:JVI.00676-08 [pii]10.1128/JVI.00676-08 (2008).

30 Millet, J. K. & Whittaker, G. R. Host cell entry of Middle East respiratory syndrome coronavirus after two-step, furin-mediated activation of the spike protein. *Proc Natl Acad Sci U S A* **111**, 15214-15219, doi:10.1073/pnas.1407087111 (2014).

31 Park, J. E. *et al.* Proteolytic processing of Middle East respiratory syndrome coronavirus spikes expands virus tropism. *Proc Natl Acad Sci U S A* **113**, 12262-12267, doi:10.1073/pnas.1608147113 (2016).

32 de Lartigue, J. *et al.* PIKfyve regulation of endosome-linked pathways. *Traffic* **10**, 883-893, doi:10.1111/j.1600-0854.2009.00915.x (2009).

33 Rutherford, A. C. *et al.* The mammalian phosphatidylinositol 3-phosphate 5-kinase (PIKfyve) regulates endosome-to-TGN retrograde transport. *J Cell Sci* **119**, 3944-3957, doi:10.1242/jcs.03153 (2006).

34 Nelson, E. A. *et al.* The phosphatidylinositol-3-phosphate 5-kinase inhibitor apilimod blocks filoviral entry and infection. *PLoS Negl Trop Dis* **11**, e0005540, doi:10.1371/journal.pntd.0005540 (2017).

35 Li, P., Gu, M. & Xu, H. Lysosomal Ion Channels as Decoders of Cellular Signals. *Trends Biochem Sci* **44**, 110-124, doi:10.1016/j.tibs.2018.10.006 (2019).

36 Sakurai, Y. *et al.* Ebola virus. Two-pore channels control Ebola virus host cell entry and are drug targets for disease treatment. *Science* **347**, 995-998, doi:10.1126/science.1258758 (2015).

37 Diehl, W. E. *et al.* Ebola Virus Glycoprotein with Increased Infectivity Dominated the 2013-2016 Epidemic. *Cell* **167**, 1088-1098 e1086, doi:10.1016/j.cell.2016.10.014 (2016).

38 Urbanowicz, R. A. *et al.* Human Adaptation of Ebola Virus during the West African Outbreak. *Cell* **167**, 1079-1087 e1075, doi:10.1016/j.cell.2016.10.013 (2016).

39 Wang, M. K., Lim, S. Y., Lee, S. M. & Cunningham, J. M. Biochemical Basis for Increased Activity of Ebola Glycoprotein in the 2013-16 Epidemic. *Cell host & microbe* **21**, 367-375, doi:10.1016/j.chom.2017.02.002 (2017).

40 Li, F. Receptor Recognition Mechanisms of Coronaviruses: a Decade of Structural Studies. *J Virol* **89**, 1954-1964, doi:10.1128/JVI.02615-14 (2015).

41 Menachery, V. D. *et al.* SARS-like WIV1-CoV poised for human emergence. *Proc Natl Acad Sci U S A* **113**, 3048-3053, doi:10.1073/pnas.1517719113 (2016).

42 Vorou, R. M., Papavassiliou, V. G. & Tsiodras, S. Emerging zoonoses and vector-borne infections affecting humans in Europe. *Epidemiol Infect* **135**, 1231-1247, doi:10.1017/S0950268807008527 (2007).

43 WHO. Novel Coronavirus (2019-nCoV) situation reports. https://www.who.int/docs/default-source/coronaviruse/situation-reports/20200210-sitrep-21-ncov.pdf?sfvrsn=947679ef_2. (2020).

44 Park, Y. J. *et al.* Structures of MERS-CoV spike glycoprotein in complex with sialoside attachment receptors. *Nature structural & molecular biology* **26**, 1151-1157, doi:10.1038/s41594-019-0334-7 (2019).

45 Hulswit, R. J. G. *et al.* Human coronaviruses OC43 and HKU1 bind to 9-O-

acetylated sialic acids via a conserved receptor-binding site in spike protein domain A. *Proc Natl Acad Sci U S A* **116**, 2681-2690, doi:10.1073/pnas.1809667116 (2019).

46 Huang, X. *et al.* Human Coronavirus HKU1 Spike Protein Uses O-Acetylated Sialic Acid as an Attachment Receptor Determinant and Employs Hemagglutinin-Esterase Protein as a Receptor-Destroying Enzyme. *J Virol* **89**, 7202-7213, doi:10.1128/JVI.00854-15 (2015).

47 Simmons, G. *et al.* Inhibitors of cathepsin L prevent severe acute respiratory syndrome coronavirus entry. *Proc Natl Acad Sci U S A* **102**, 11876-11881, doi:0505577102 [pii]10.1073/pnas.0505577102 (2005).

48 Li, P. *et al.* Identification of H209 as Essential for pH 8-Triggered Receptor-Independent Syncytium Formation by S Protein of Mouse Hepatitis Virus A59. *J Virol* **92**, doi:10.1128/JVI.00209-18 (2018).

49 Gunaratne, G. S., Yang, Y., Li, F., Walseth, T. F. & Marchant, J. S. NAADP-dependent Ca(2+) signaling regulates Middle East respiratory syndrome-coronavirus pseudovirus translocation through the endolysosomal system. *Cell Calcium* **75**, 30-41, doi:10.1016/j.ceca.2018.08.003 (2018).

50 Ou, X. *et al.* Identification of the Fusion Peptide-Containing Region in Betacoronavirus Spike Glycoproteins. *J Virol* **90**, 5586-5600, doi:10.1128/JVI.00015-16 (2016).

51 Mi, D. *et al.* Glycine 29 Is Critical for Conformational Changes of the Spike Glycoprotein of Mouse Hepatitis Virus A59 Triggered by either Receptor Binding or High pH. *J Virol* **93**, doi:10.1128/JVI.01046-19 (2019).

Table

Table 1. Neutralization activities of antisera from SARS-CoV and 2019-nCoV patients.

qPatient serum	SARS-CoV S pseudovirion	2019-nCoV S pseudovirion
SARS-CoV patient	>80	40
2019-nCoV patient #1	Not detected	>80
2019-nCoV patient #2	Not detected	40
2019-nCoV patient #3	Not detected	80
2019-nCoV patient #4	Not detected	>80
2019-nCoV patient #5	Not detected	>80

SARS-CoV and 2019-nCoV S pseudovirions were pre-incubated with serially diluted patient sera for 1 hour on ice, then virus-antibody mixture was added on 293/hACE2 cells. Cells were lysed 40 hours later and pseudovirus transduction was measured. The highest dilution of the serum sample that decreased transduction by 50% or more was considered to be positive

Figures

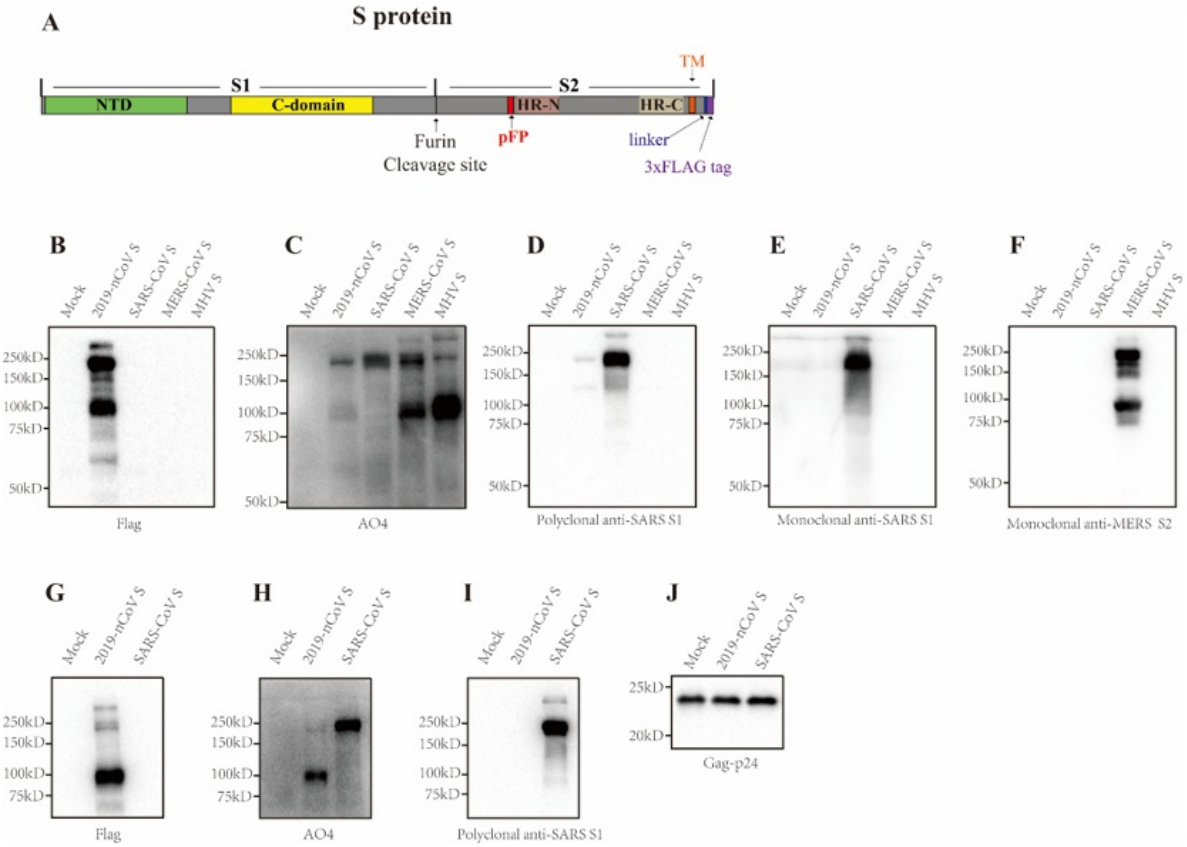

Figure 1

Incorporation of 2019-nCoV S protein into pseudovirions. (A) Diagram of full length 2019-nCoV S protein with a 3xFLAG tag. S1, receptor binding subunit; S2,

membrane fusion subunit; TM, transmembrane domain. (B-F)Detection of CoVs S protein in cells lysate by western blot. Mock, 293T cells transfected with empty vector. (B) Mouse monoclonal anti-FLAG M2 antibody; (C) Polyclonal goat anti-MHV-A59 S protein antibody AO4. (D) Polyclonal rabbit anti-SARS S1 antibodies T62. (E) Mouse monoclonal anti-SARS S1 antibody. (F) Mouse monoclonal anti-MERS-CoV S2 antibody. (G-J) Detection of CoVs S protein in pseudovirions by western blot .Gag-p24 served as a loading control. (G) Anti-FLAG M2. (H) AO4. (I) Polyclonal rabbit anti-SARS S1 antibodies T62. (J) Polyclonal anti-Gag-p24 antibodies. uncleaved S protein, about 180 kDa; cleaved S protein, about 90 kDa..Experiments were done twice and one is shown.

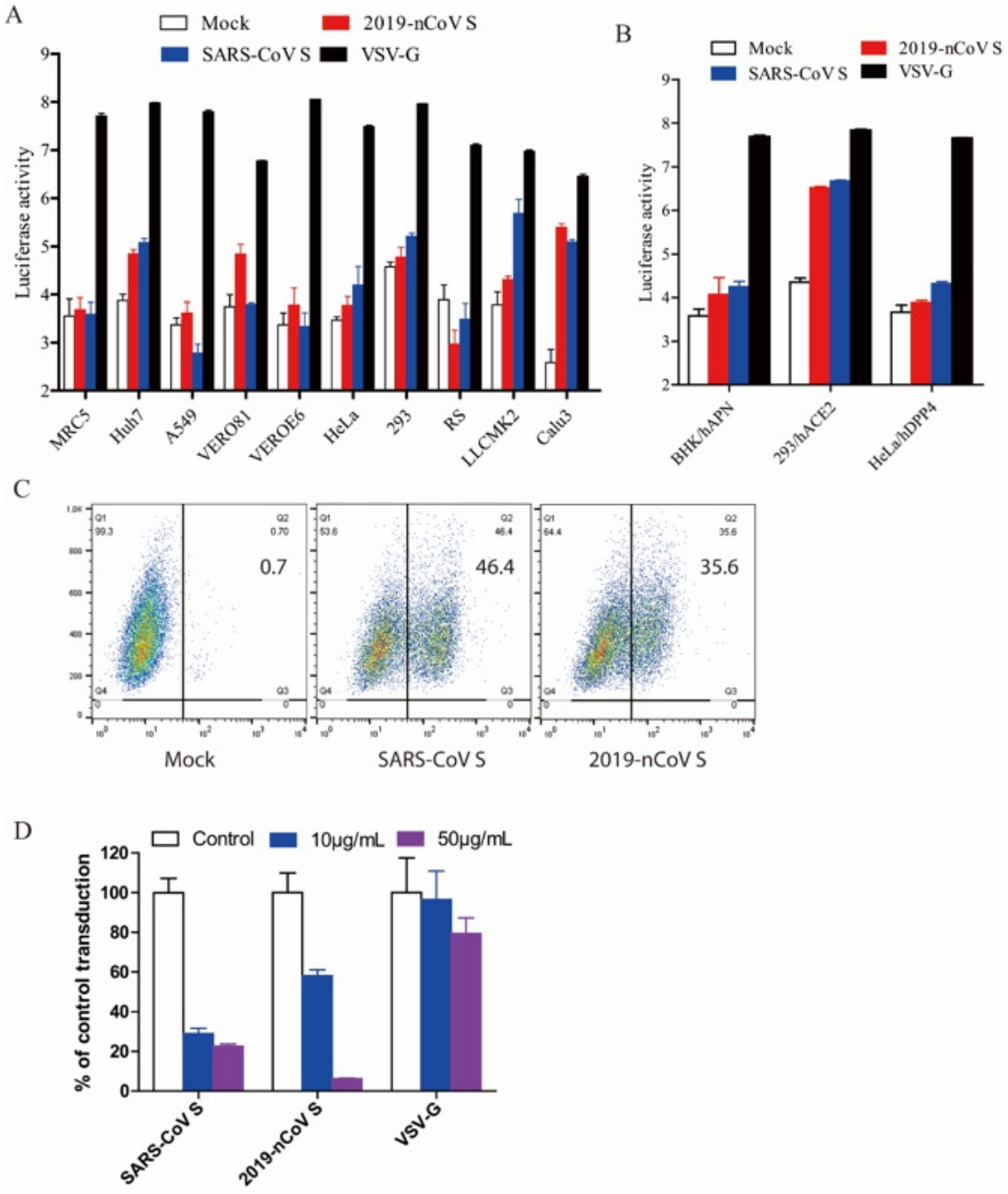

Figure 2

Entry of 2019-nCoV S pseudovirons on different cell type and identification of hACE2 as the receptor for 2019-nCoV. (A) (B) Entry of SARS-CoV S pseudovirions on indicated cell lines. Cells from human and animal origin were inoculated with 2019-nCoV S (red), SARS-CoV S (blue), or VSV-G (black) pseudovirions. At 48hrs postinoculation, transduction efficiency was measured according to luciferase

activities. RS, Rhinolophus sinicus bat embryonic fibroblast; BHK/hAPN, BHK cells stably expressing hAPN, the hCoV-229E receptor; 293/hACE2, 293 cells stably expressing hACE2, the SARS-CoV receptor; HeLa/hDPP4, HeLa cells stably expressing hDPP4, the MERS-CoV receptor. Experiments were done triplicate and repeated at least three times. One representative is shown with error bars indicate SEM. (C) Binding of SARS-CoV S and 2019-nCoV S proteins to soluble hACE2. HEK293T cells transiently expressing SARS-CoV and 2019-nCoV S proteins were incubated with the soluble hACE2 on ice, followed by polyclonal goat anti-hACE2 antibody. Cells were analyzed by flow cytometry. The experiments were repeated at least three times. (D) Inhibition of 2019-nCoV S pseudovirion entry by soluble hACE2. SARS-CoV S, 2019-nCoV S, or VSV-G pseudovirions were pre-incubated with soluble hACE2, then mixture were added to 293/hACE2 cells. Cells were lysed 40 hrs later and pseudoviral transduction was measured. Experiments were done twice and one is shown.

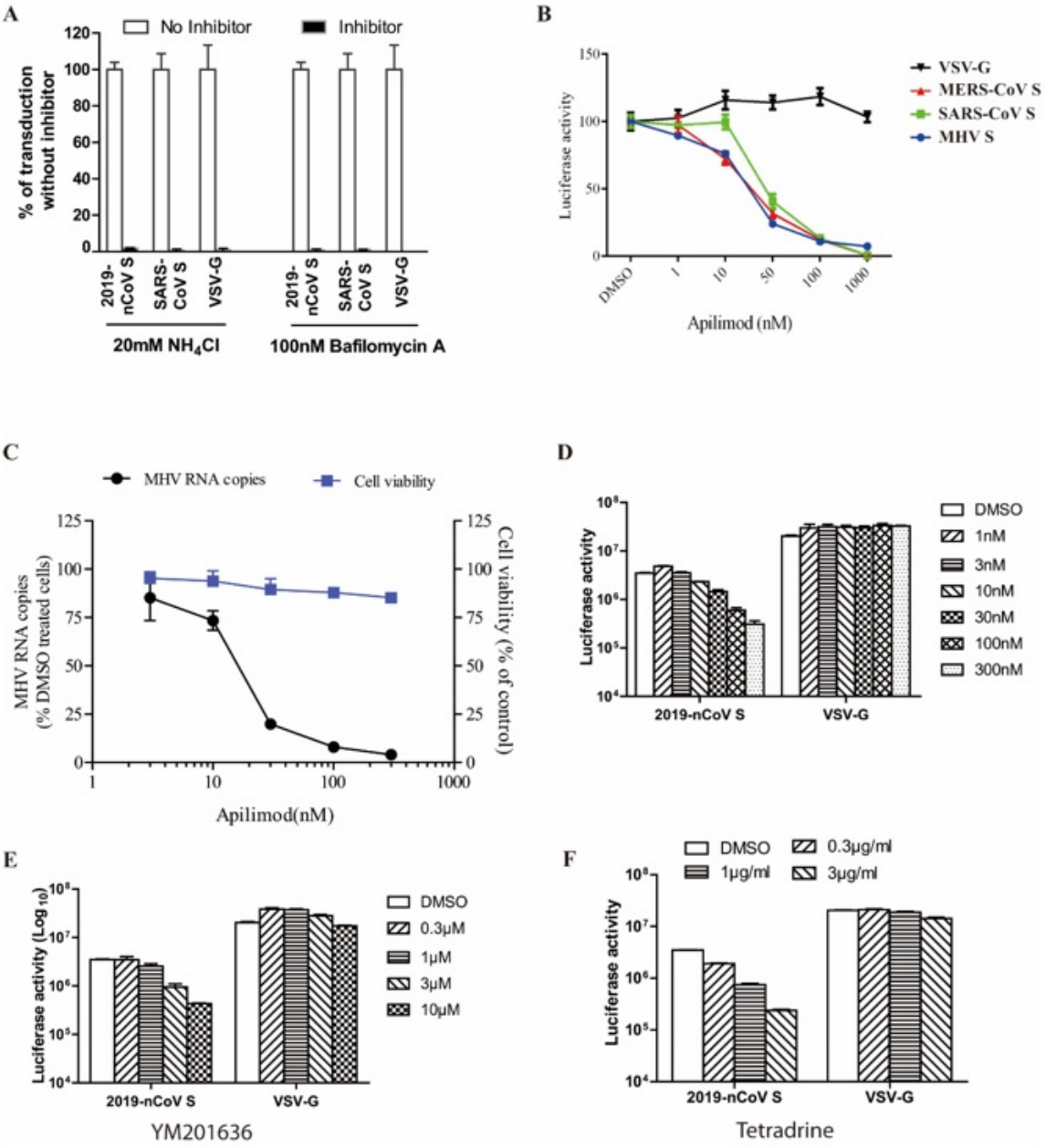

Figure 3

The 2019-nCoV S pseudovirions enter 293/hACE2 cells through endocytosis. (A) Inhibition of entry of 2019-nCoV S pseudovirion on 293/hACE2 by lysosomotropic agents (20mM NH4Cl and 100nM bafilomycin A). (B) Inhibition of entry of SARS-CoV, MERS-CoV, and MHV S pseudovirions by a PIKfyve inhibitor apilimod. HeLa/mCEACAM, 293/hACE2, HeLa/hDPP4 cells were pretreated with different concentrations of apilimod and transduced with MHV S, SARS-CoV S, MERS-CoV S

pseudovirions, respectively. The luciferase activity was measured 40 hrs post transduction. VSV-G pseudovirions were used as a control. Experiments were done triplicate and repeated at least three times. One representative is shown with error bars indicate SEM. (C) Inhibition of MHV A59 infection by apilimod. The 17Cl.1 cells were pretreated with 3, 10, 30, 100, 300nM apilimod for 30 min and infected by MHV A59 at MOI=0.01. Viral infection and cell viability were determined by using qPCR and MTT assay, respectively. Experiments were done triplicate and repeated at least three times. One representative is shown with error bars indicate SEM. (D-E) Inhibition of entry of 2019-nCoV S protein pseudovirions by apilimod, YM201636, and tetrandrine. HEK 293/hACE2 cells were pretreated with either apilimod (D), YM201636 (E), or tetrandrine (F), then inoculated with 2019-nCoV S pseudovirons in the presence of drug. The luciferase activity were measured 40 hrs post transduction. YM201636, PIKfyve inhibitor; tetradrine, TPC2 inhibitor. The experiments were done triplicate and repeated at least three times.

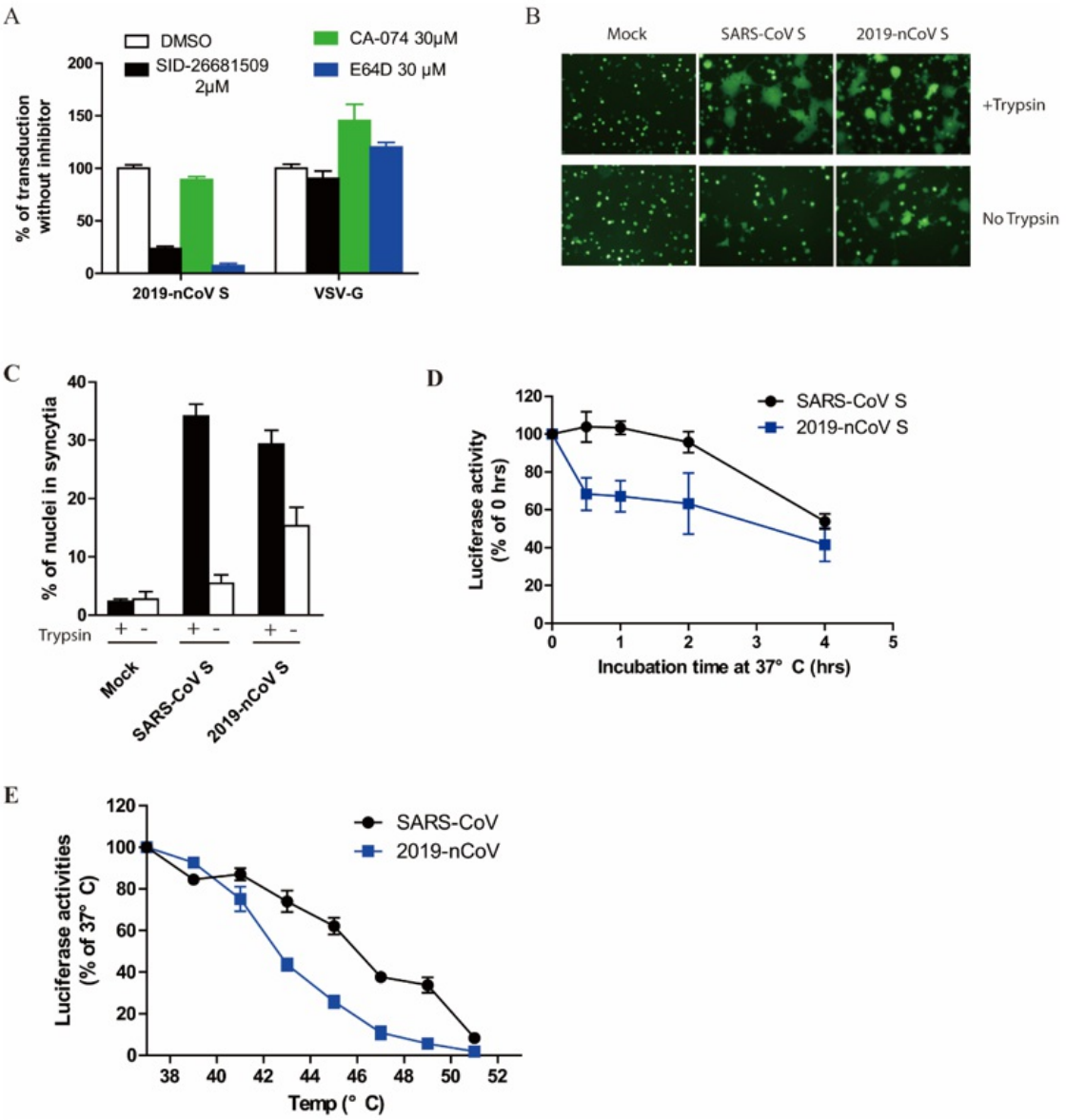

Figure 4

Activation of 2019-nCoV S protein by cathepsin and trypsin. (A). Effects of cathepsin inhibitors on entry of 2019-nCoV S pseudovirions on 293/hACE2 cells. HEK 293/hACE2 cells were pretreated with broad spectrum cathepsin inhibitor E64D, cathepsin L-specific inhibitor (SID 26681509), or cathepsin B-specific inhibitor (CA-074) and then transduced with 2019-nCoV S and VSV-G pseudovirions. Pseudoviral transduction was measured at 40 hrs post-inoculation. Experiments were done triplicate and repeated at least three times. One

representative is shown with error bars indicate SEM. (B) Cell-cell fusion mediated by 2019-nCoV S protein. HEK 293T cells were transiently expressing eGFP and either 2019-nCoV or SARS-CoV S protein were detached with either trypsin or EDTA, and co-cultured with 293/hACE2 or 293 cells for 4 hrs at 37℃. (C) Quantitative analysis of syncytia in panel B. (D) (E) Thermostability analysis of 2019-nCoV S protein. (D) SARS-CoV and 2019-nCoV S pseudovirons were incubated at 37°C for the specified times (0 to 4 hrs) in the absence of serum, and then assayed on 293/hACE2 cells. The results from infection at 0 h were set as 100%, and the experiments were repeated four times. (E) SARS-CoV and 2019-nCoV S pseudovirions without serum were incubated at the indicated temperature (37 to 51°C) for 2 hrs and then assayed on 293/hACE2 cells. The results are reported as the percentage of transduction at 37°C. The experiments were repeated four times, and means with standard deviations are shown.

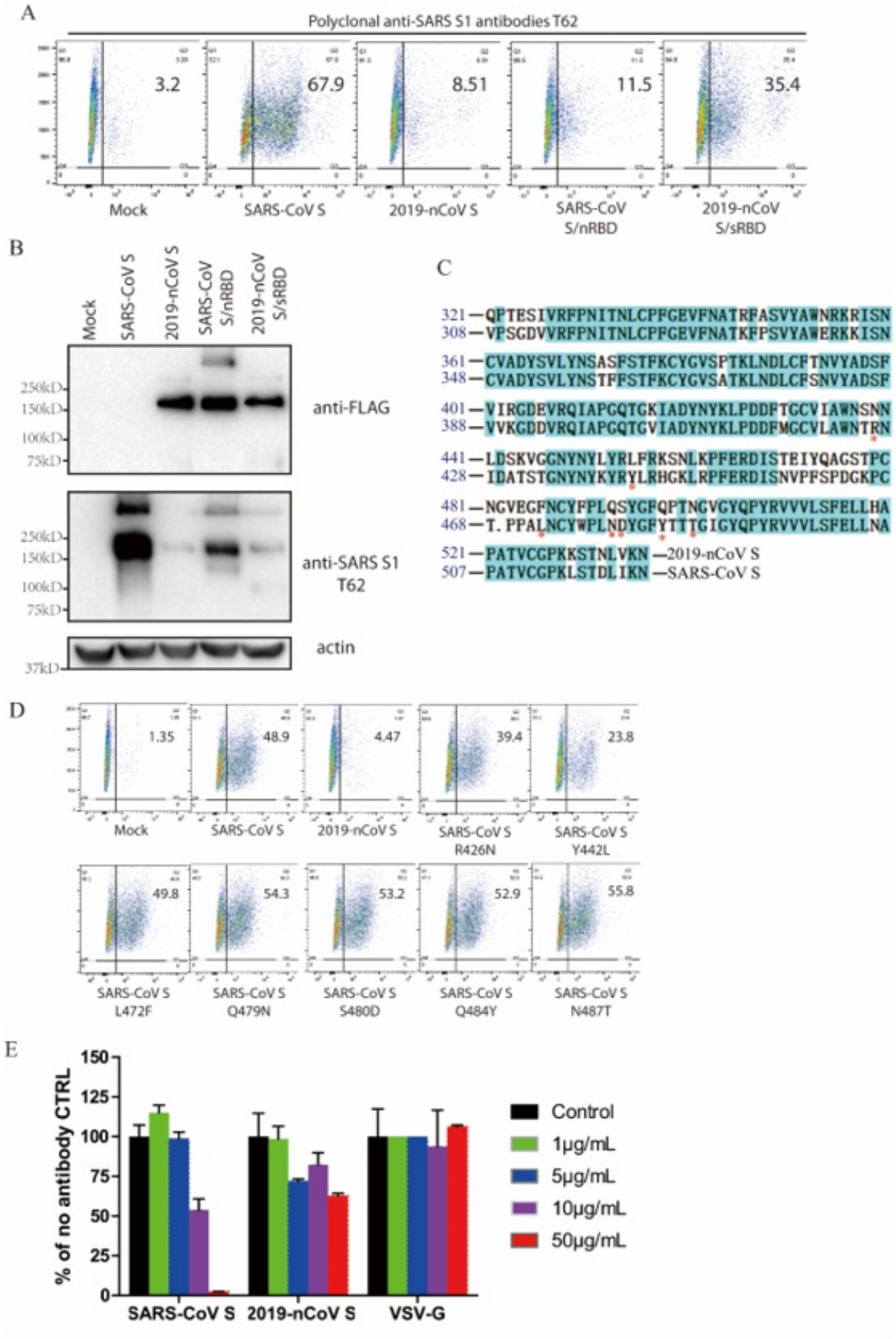
A
Polyclonal anti-SARS S1 antibodies T62
3.2
67.9
8.51
11.5
35.4
Mock
SARS-CoV S
2019-nCoV S
SARS-CoV S/nRBD
2019-nCoV S/sRBD
B
Mock
SARS-CoV S
2019-nCoV S
SARS-CoV S/nRBD
2019-nCoV S/sRBD
250kD
150kD
100kD
75kD
anti-FLAG
anti-SARS S1 T62
actin
37kD
C
321 — QPTESIVRFPNITNLCPFGEVFNATRFASVYAWNRKRISN
308 — VPSGDVVRFPNITNLCPFGEVFNATKFPSVYAWERKKISN
361 — CVADYSVLYNSASFSTFKCYGVSPTKLNDLCFTNVYADSF
348 — CVADYSVLYNSTFFSTFKCYGVSATKLNDLCFSNVYADSF
401 — VIRGDEVRQIAPGQTGKIADYNYKLPDDFTGCVIAWNSNN
388 — VVKGDDVRQIAPGQTGVIADYNYKLPDDFMGCVLAWNTRN
441 — LDSKVGGNYNYLYRLFRKSNLKPFERDISTEIYQAGSTPC
428 — IDATSTGNYNYKYRYLRHGKLRPFERDISNVPFSPDGKPC
481 — NGVEGFNCYFPLQSYGFQPTNGVGYQPYRVVVLSFELLHA
468 — T. PPALNCYWPLNDYGFYTTTGIGYQPYRVVVLSFELLNA
521 — PATVCGPKKSTNLVKN — 2019-nCoV S
507 — PATVCGPKLSTDLIKN — SARS-CoV S
D
1.35
48.9
4.47
39.4
23.8
Mock
SARS-CoV S
2019-nCoV S
SARS-CoV S R426N
SARS-CoV S Y442L
49.8
54.3
53.2
52.9
55.8
SARS-CoV S L472F
SARS-CoV S Q479N
SARS-CoV S S480D
SARS-CoV S Q484Y
SARS-CoV S N487T
E
% of no antibody CTRL
150
125
100
75
50
25
0
SARS-CoV S
2019-nCoV S
VSV-G
Control
1μg/mL
5μg/mL
10μg/mL
50μg/mL

Figure 5

Characterization of polyclonal rabbit anti-SARS S1 antibodies T62 on 2019-nCoV and SARS-CoV S proteins. (A)Binding of polyclonal rabbit anti-SARS S1 antibodies T62 to 2019-nCoV, SARS-CoV S, and chimeric S proteins. HEK 293T cells transiently expressing either 2019-nCoV S, SARS-CoV S, SARS-CoV S/nRBD, or 2019-nCoV S/sRBD proteins were incubated with polyclonal rabbit anti-SARS-CoV S1 antibody T62 for 1 h on ice, followed by a FITC-conjugated secondary antibody, then cells were analyzed by flow cytometry. Experiments were done three times and one representative is shown. (B) Expression of 2019-nCoV S, SARS-CoV S, or chimeric S proteins on 293T cells. Cells from panel A were lyzed and blotted with anti-FLAG M2 antibody and polyclonal anti-SARS S1 antibody T62. (C) Amino acid sequence alignment of SARS-CoV and 2019-nCoV S RBDs. Stars (*) indicate the seven critical residues different between 2019-nCoV and SARS-CoV RBDs. (D) Binding of polyclonal rabbit anti-SARS S1antibodies T62 to mutant SARS-CoV S proteins. (E) Neutralization of 2019-nCoV S and SARS-CoV S pseudovirions by polyclonal rabbit anti-SARS S1 antibody T62. Pseudovirons were pre-incubated with serially diluted polyclonal rabbit anti-SARS S1 antibodies T62 on ice, then virus-antibody mixture was added on 293/hACE2 cells. Pseudoviral transduction was measured 40 hrs later. Experiment was done in triplicate and repeat twice, and one representative is shown.

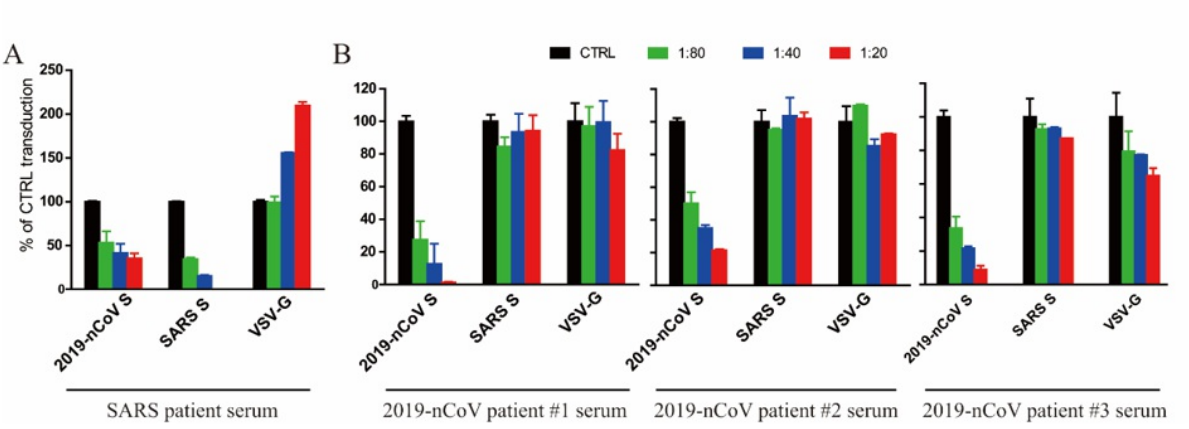

Figure 6

Neutralization of 2019-nCoV S and SARS-CoV S pseudovirions by sera from recovered SARS-CoV patient and 2019-nCoV patients. All sera were incubated on 56℃ for 30 min to eliminate complement. SARS-CoV S and 2019-nCoV S pseudovirons were pre-incubated with serially diluted SARS patient serum (A) or 2019-nCoV patient sera (B) for 1 h on ice and then added on 293/hACE2 cells. Pseudoviral transduction was measured 40 hrs later. Experiment were done in triplicate and repeat twice. One representative is shown.

Supplementary Files

This is a list of supplementary files associated with the primary manuscript. Click to download.

Fig S1.pdf
Fig S2.pdf
Fig S3.pdf